JOURNAL OF OPTOELECTRONICS AND ADVANCED MATERIALS, Vol. 10, No. 12, December 2008, p. 3165 - 3168

Experimental and theoretical investigation of optical properties of colloidal photonic crystal films

C. FARCĂU[a,b], E.VINȚELER[a*], S. AȘTILEAN[a,b]
[a]*Faculty of Physics, Babeş-Bolyai University, Str M. Kogalniceanu 1, 400084 Cluj-Napoca, Romania*
[b]*Nanobiophotonics Laboratory, Institute for Interdisciplinar Experimental Research, Babes-Bolyai University, T. Laurian 42, 400271, Cluj-Napoca, Romania*

We studied the experimental and calculated transmission and reflectivity spectra of a monolayer and a bilayer of periodic array of polystyrene spheres (triangular lattice) on finite glass substrate at normal incidence. We also investigated the near-field intensity $|E_x|^2$ at different relevant wavelengths for a sampling plane that crosses the monolayer of spheres at equator. We find that transmission and reflectivity minima are related to near-field coupling between neighbouring spheres, forming waveguide photonic modes of the array.

(Received October 30, 2008; accepted November 27, 2008)

Keywords: Colloidal photonic crystals, Finite-difference time-domain

1. Introduction

The optical properties of photonic band gap materials have been the subject of many experimental and theoretical studies in recent years [1,2]. In these systems the dielectric function is spatially periodic in one or more dimensions, with the period comparable to the light wavelength. As a result, their optical properties are dominated by strong diffraction effects, light propagation being strongly inhibited over a narrow range of frequencies. This is observed experimentally as a dip in the transmission spectrum, along selected directions (photonic pseudogap) or along all the directions (full photonic band gap).

Recently, colloidal photonic crystal films made of mono- or multi-layers of dielectric (polystyrene) nano-(micro)spheres received increasing attention because such structures could be used as planar defects in three dimensional photonic structures [3] or templates for the creation of metal-dielectric hybrid architectures [4] with plasmonic applications. A good understanding for the evolution of the optical properties of these materials as function of number of layers is still lacking in literature.

In this work, we study the optical properties of colloidal photonic crystal films consisting of one and two layers of close-packed mono-disperse polystyrene spheres of 400 nm diameter. We study their transmission and reflectivity in visible light at normal incidence, both theoretically and experimentally. Furthermore, we compute and compare the local field intensity $|E_x|^2$ inside the film in two relevant photonic regimes, i.e. *in resonance* and *out of resonance,* at λ=480 nm and λ= 600 nm, respectively.

2. Sample fabrication

The colloidal crystal films were fabricated via a convective assembly technique, by using a home-built apparatus [5]. A droplet of water containing polystyrene spheres (PS) of 400 nm diameter was injected into the wedge between a substrate slide and a deposition slide which is positioned in close proximity with the substrate and tilted by an angle of 27°. As the deposition slide was translated across the substrate, a 2D array of PS self-organized on the substrate due to water evaporation and particles flow from the solution towards the meniscus.

Thickness of the colloidal crystal film, i.e. number of layers, is controlled by adjusting the deposition speed (translation speed of deposition slide) to the concentration of polymer spheres in solution and sphere diameter.

We inspected the crystallinity of the obtained colloidal films by optical microscopy and scanning electron microscopy (SEM). The optical properties were investigated by using a Jasco V-530 uv-vis spectrophotometer working with unpolarized light. Reflectivity measurements were performed on the same apparatus by using an interchangeable Jasco SLM-468S reflectivity module.

3. Modeling

Numerical simulations were performed using a finite difference time-domain (FDTD) method [6-8], by means of a freely available software package MEEP (downloadable at MIT site) with subpixel smoothing for increased accuracy [9]. The simulation model propagation of electromagnetic waves using discretized Maxwell's equations in three dimensions taking into account both material shape and dispersion. As shown in Fig. 1, the rectangular computational cell used had dimensions of *a x*

b x c grid points, where *a=30, b=52* are the horizontal lattice constants (in grid points - GP) of the hexagonal packing period, and every grid point GP corresponds to 13.33 nm. The vertical size of cell *c* depends on the number of layers and for 2 layers it is 310 grid points. The layers of polystyrene spheres (n = 1.56) with diameter of 400 nm were placed in the middle of the computational cell, and were surrounded by air on one side, and a half space of glass substrate on the other.

A temporally Gaussian pulse was incident normally on the polystyrene spheres layers from the air side. Perfectly matched layer (PML) boundary conditions [10,11] were applied on the boundaries normal to the incident light to prevent reflections (vertical direction), and periodic boundary conditions were applied in the other directions (horizontal directions). The electromagnetic fields at planes located on both sides of the polystyrene spheres layers just before the PMLs were recorded and the Poynting power fluxes were calculated from the discrete Fourier transforms of the fields. This power must be normalized to the incident flux and this implies to repeat the simulation with and without the polystyrene spheres layers. The transmissivity $T^A_{\ layer}$ is given by the ratio of the flux through the plane with the layer, over the flux through the same plane, but in the case without the layer. The calculation for the reflectivity $R^A_{\ layer}$ is similar, although in this case the incident and reflected fields need to be separated before calculating the flux. The same procedure and calculations must be performed when we calculate $T^G_{\ layer}$ and $R^G_{\ layer}$. In this case the Gaussian pulse propagates from the glass side.

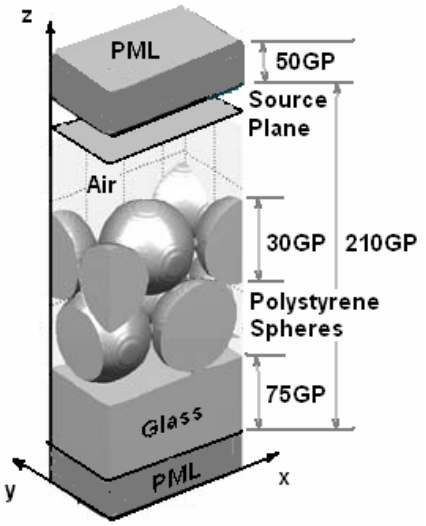

Fig.1. Schematic representation of the computational cell for 2 layers of polystyrene spheres.

The transmission through and reflection from the glass substrate alone were calculated using a wave optics formulation. The layers of polystyrene spheres were modeled as sandwiched between two infinite half-spaces of air (*n = 1*) and glass (*n = 1.5*), resulting in the transmissivity $T_{layer}(\omega)$, and reflectivity $R_{layer}(\omega)$ of the layer alone. On the other side of the glass next to air, Fresnel coefficients were used to calculate the corresponding quantities, T_{glass}=0.96 and R_{glass}=0.04. Ray tracing of the intensity through the glass substrate is then used to calculate the transmission through the entire structure (see Fig. 2).

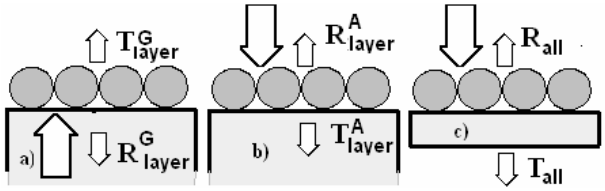

Fig. 2 Transmissivity and reflectivity a) for incident light from glass side b) for incident light from air side c) for incident light on finite thickness glass substrate

The overall transmission and reflection are given by:

$$T_{all}(\omega)= T^A_{\ layer}(\omega)* T_{glass}/(1- R^A_{\ layer}(\omega)*R_{glass}), \quad (1)$$

$$R_{all}(\omega)= R^A_{\ layer}(\omega)+ T^A_{\ layer}(\omega)* T^G_{\ layer}(\omega)*R_{glass}/ /(1- R^A_{\ layer}(\omega)*R_{glass}) \quad (2)$$

where we distinguish between the case when incident light is coming first from air (label A) or from glass (label G).

4. Results

Conventional optical microscopy allows us to distinguish between one-, two- or multi-layer structure colloidal films. We obtained selectively mono- or bi-layer colloidal films by decreasing the deposition speed from 30 to 17 μm/s, at 10 vol.% colloidal solution concentration.

Fig. 3 shows a representative scanning electron microscopy (SEM) image of the two-dimensional array of polystyrene spheres. Even if the prepared sample is polycrystalline, it has domains of different orientations, we usually find monocrystalline regions of hundreds square micrometers areas. The inset in figure 3 is a zoom in the same area, in which a point defect (missing sphere) reveals the PS underlayer and also the close-packed crystal structure.

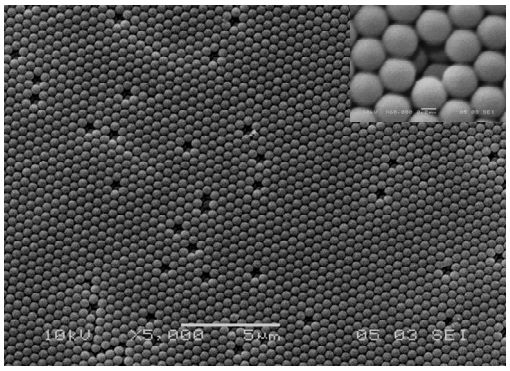

Fig.3. Scanning electron microscopy image of a two-layer colloidal crystal film; inset is a zoom revealing the layer below and the crystal structure.

Shown in Fig. 4-5 are the measured and simulated transmission and reflectivity spectra of 1 and 2 layers (hexagonal packing) of polystyrene spheres with diameter of 400 nm on 1 mm glass substrate.

When we compare theory with experiment (see fig. 4-5) we observe two differences:

The experimental transmission falls slowly when we pass from high to low wavelengths due to absorption in glass substrate (significant for wavelengths under 0.46 μm) and polystyrene sphere layers (non-zero for wavelengths under 0.39 μm). The simulation does not take in account this absorption and the theoretical transmission is on average at the same level.

We observe that the experimental transmission is smeared at the first dip (λ = 0.477 μm) compared to the theoretical transmission and we have the following explanations: in experiment the light is transmitted through a square region containing 5000x5000 polystyrene spheres and, unfortunately this is not a perfect photonic crystal (as it is in simulations). We have a network of tree-like defects - a usual picture in real crystals - that modifies reflectivity and transmittance.

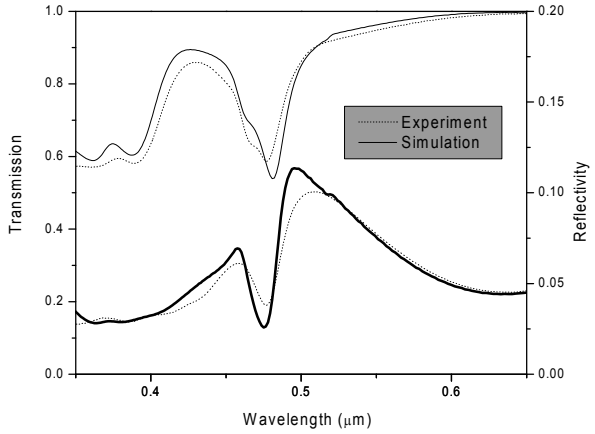

Fig. 4. Transmission (up) and reflectivity spectra (down) for a monolayer of polystyrene spheres with diameter a=0.4 μm on glass substrate.

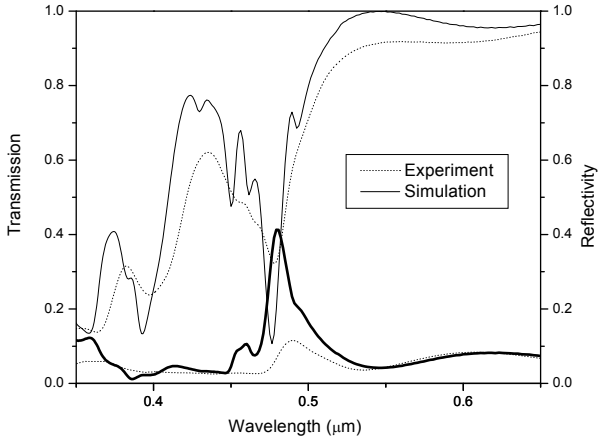

Fig. 5. Transmission (up) and reflectivity spectra (down) for a bi-layer of polystyrene spheres with diameter a=0.4 μm on glass substrate.

Though we have these problems in comparing theory with experiment, the interesting point is that the simulated frequency at which transmission and reflectivity falls (the first dip at λ = 0.477 μm or at dimensionless parameter Z = $\sqrt{3}a/2\lambda$ = 0.70) is only mildly affected by all these intricacies. The same is true also for the second dip in transmission and reflectivity at λ = 0.393 μm (or Z = 0.88).

Our computations give similar results for transmission and reflectivity spectra of a monolayer of spheres with those calculated using another method based on expansion of Bloch electromagnetic field in terms of spherical waves [12,13]. In their papers they gave complete results without substrate and only the transmission spectrum in the presence of a dielectric substrate. Their simulated first degenerate dip in transmission is at Z = 0.70 (they considered spheres with dielectric permittivity ε_Q = 2.56 on semi-infinite substrate with ε_S = 2.28 close to our value ε_Q = 2.4336 and ε_S = 2.25) and we have two dips at Z = 0.721 (λ = 0.48 μm) and Z = 0.739 (λ = 0.468 μm). Their second dip is at Z = 0.85 and in our case Z = 0.88 and λ = 0.393 μm. Our simulated reflectivity has a dip at Z = 0.70 (λ = 0.477 μm) and two peaks at Z =0.692 (λ = 0.5 μm) and Z = 0.744 (λ = 0.465 μm).

For a bilayer of spheres we have three dips in transmission at Z =0.723, 0.74, 0.759 (λ = 0.479, 0.469, 0.459 μm) and two peaks in reflectivity at Z =0.718, 0.74 (λ = 0.482, 0.469 μm) and one dip in reflectivity at Z =0.729 (λ = 0.475 μm).

5. Discussion

An observation that has to be emphasized is that the minimum in transmission coincides with a reflectivity minimum. If one calculates 1-T-R, an inferred absorption, finds that at resonant wavelength a certain amount of the incident flux is missing.

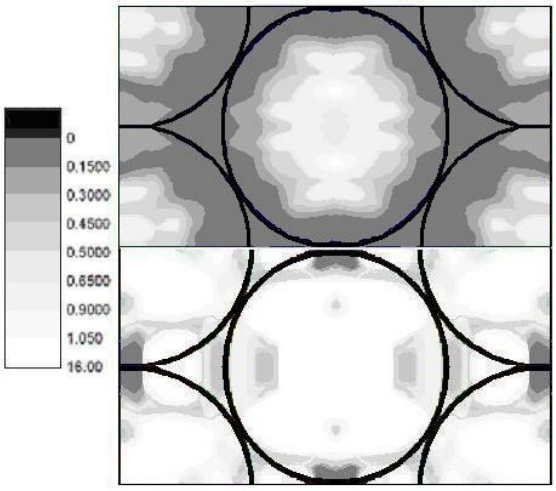

Fig. 6. Contour plots of local field intensity $|E_x|^2$ in two photonic regimes: out of resonance (at λ=0.6 μm - up) and in resonance (at λ=0.48 μm - down) for a monolayer of polystyrene spheres on glass substrate. The sampling plane crosses the spheres at equator (black curves show the circumferences of the spheres).

To understand better the photonic behaviour at these wavelengths we computed in Fig. 6 the local field intensity $|E_x|^2$ in two photonic regimes: out of resonance (at λ=0.6 μm) and in resonance (at λ=0.477 μm) for monolayer of polystyrene spheres on glass substrate. The sampling plane crosses the spheres at equator (black curves show the circumferences of the spheres) and incident light has only one component E_x parallel with axis x as indicated in Fig. 1. Out of resonance we observe only isolated isles formed by the field intensity indicating that the incident flux is not propagating in the horizontal layer of polystyrene spheres. But in the region *in resonance,* the field intensity forms a connected network that allows the horizontal propagation of incident flux and the fall of transmittance in vertical direction.

6. Conclusions

The measured and simulated transmission and reflectivity in visible light at normal incidence are in good agreement, especially the positions of dips. We found that the PS monolayer acts as a photonic waveguide for wavelengths matching the periodicity of the array and polystyrene dielectric constant.

The dip in transmission is due to light waves traveling in the plane of the polystyrene spheres layer, thus forming a standing-wave pattern of six-fold symmetry. Effects of coupling between photons traveling in the bottom layer and those traveling in the upper layer are still under investigation.

Acknowledgements

This research was supported by the Romanian Agency for Scientific Research under the project CEEX 71/2006 (Nanobiospec).

References

[1] K. Sakoda, Optical properties of photonic crystals, Springer, (2001).
[2] E. Pavarini, L.C. Andreani, C. Soci, M. Galli, F. Marabelli, D. Comoretto, Phys. Rev. B, **72**, 045102 (2005).
[3] S. Wong, V. Kitaev, G.A. Ozin, J. Am. Chem. Soc., **125**, 15589 (2003).
[4] C. Farcau, S. Astilean, J. Opt. A: Pure Appl. Opt., **9**, S345 (2007).
[5] A. Kuttesch, C. Farcau, Z. Neda, S. Astilean, Proc. SPIE, **6785**, 678500 (2007).
[6] A. Taflove and S. C. Hagness, Computational Electrodynamics: The Finite-Difference Time-Domain Method, 3rd ed. Artech House, Norwood, MA, (2000).
[7] J. D. Joannopoulos, R. D. Meade, and J. N. Winn, Photonic Crystals, Princeton University Press, Princeton, NJ, (1995).
[8] S. G. Johnson and J. D. Joannopoulos, Photonic Crystals: The Road from Theory to Practice, Kluwer, Boston, (2002).
[9] A. Farjadpour, D. Roundy, A. Rodriguez, M. Ibanescu, P. Bermel, J. D. Joannopoulos, S.G. Johnson, G. Burr, Optics Letters **31**, 2972 (2006).
[10] P. Lalanne, E. Silberstein, Opt. Lett. **25**, 1092 (2000).
[11] E. Silberstein, P. Lalanne, J.-P. Hugonin, and Q. Cao, J. Opt. Soc. Am. A **18**, 2865 (2001).
[12] H.Miyazaki, K. Ohtaka, Phys.Rev. B **58**, 6920 (1998).
[13] Y.Kurokawa, H.Miyazaki, Y. Jimba, Phys.Rev. B **65**, 201102 (2002).

*Corresponding author: evinteler@phys.ubbcluj.ro